Vietnam Journal of Mechanics, Vol. 46, No. 1 (2024), pp. 15 – 30
DOI: https://doi.org/10.15625/0866-7136/20575

FREQUENCY RESPONSE FUNCTION OF CRACKED TIMOSHENKO BEAM MEASURED BY A DISTRIBUTED PIEZOELECTRIC SENSOR

Nguyen Tien Khiem[1,*], Tran Thanh Hai[1], Nguyen Thi Lan[1], Ho Quang Quyet[1], Ha Thanh Ngoc[2], Pham Van Kha[3]
[1]*Institute of Mechanics, VAST, Hanoi, Vietnam*
[2]*Institute of Mechanics and Environmental Engineering, VUSTA, Hanoi, Vietnam*
[3]*HCMC Occupational Safety & Health Inspection & Training JSC, Ho Chi Minh City, Vietnam*
E-mail: ntkhiem@imech.vast.vn

Received: 20 January 2024 / Revised: 14 March 2024 / Accepted: 25 March 2024
Published online: 31 March 2024

Abstract. In the present report, a novel concept of frequency response function (FRF) is introduced for piezoelectric beam. First, a model of Timoshenko beam bonded with a piezoelectric layer is established and used for deriving the conventional frequency response function acknowledged as mechanical frequency response function (MERF). Then, the output charge produced in the piezoelectric layer is calculated from the MFRF and therefore obtained frequency-dependent function is called electrical frequency response function (EFRF) for the integrated beam. This concept of FRF depends only on exciting position and can be explicitly expressed through crack parameters. So that it provides a novel instrument to modal analysis and structural health monitoring of electro-mechanical systems, especially for crack detection in beams using distributed piezoelectric sensor. The sensitivity of EFRF to crack has been examined and illustrated in numerical examples for cracked Timoshenko beam.

Keywords: frequency response function; cracked Timoshenko beam; piezoelectric layer; sensitivity analysis.

1. INTRODUCTION

The vibration-based method (VBM) has been proven to be the most productive technique in health monitoring of engineering structures and the important results obtained recently in this field were reviewed in [1–3]. As is well known, the core problem in structural health monitoring (SHM) is detecting possible damage in a structure of interest which means identifying structure deteriorations such as cracks or debonding in layered composites. The key in the application of the VBM for SHM is choosing damage indicators that show whether a structure is damaged and the location, extent of damage if it happened. Among the damage indicators, the global (nonlocal) ones such as natural frequencies for example were first chosen because of their easily measurement but they are insensitive to local damage like cracks. The vibration mode shapes are more sensitive to local damages; however, mode shapes are more difficult to measure exactly by traditional structure testing techniques. As the original signature of natural frequencies and mode shapes, the frequency response functions have been early employed for structural damage detection problems [4–11]. However, most of the studies were based on the damage-induced changes in the FRF's shape measured still by a large number of sensors in a discretized mesh. Recently, using the piezoelectric material as components of a structure [12,13] for monitoring its condition offers an alternative technique for measuring FRFs for structural damage detection and it allows a novel technique called electro-mechanical impedance (EMI) method to be developed for SHM [14–17]. Nevertheless, the so-called EMI method is limited to investigating the electro-mechanical impedance measured with a piezoelectric transducer (sensor/actuator) in a very high-frequency range. The measured response of a structure subjected to electric excitation produced by a piezoelectric actuator in a high-frequency range often delivers weak signals to apply for structural damage detection. This drawback of the EMI technique could be overcome by using only a distributed piezoelectric sensor for measuring the frequency response of a structure subjected to mechanical excitation in the frequency range of the structure's fundamental frequency.

Thus, in the present study, a concept of frequency response function (FRF) is developed for a beam with a piezoelectric layer under mechanical excitation. First, a model of Timoshenko beam bonded with a piezoelectric layer is established and used for deriving the conventional frequency response function acknowledged as mechanical frequency response function (MERF). Then, the output charge produced in the piezoelectric layer is calculated from the MFRF and therefore obtained frequency-dependent function is called electrical frequency response function (EFRF) for the integrated beam. This concept of FRF depends only on exciting position and can be explicitly expressed through crack parameters. So that it provides a novel instrument to modal analysis and structural health monitoring of electro-mechanical systems, especially for crack detection in beams using distributed piezoelectric sensor. The sensitivity of EFRF to crack has been examined by using so-called spectral damge index [18] and illustrated in numerical examples for cracked Timoshenko beam.

2. GOVERNING EQUATIONS FOR VIBRATION OF CRACKED BEAM WITH PIEZOELECTRIC LAYER

Let us consider a Timoshenko beam of length $L_b = L$ width b and thickness h_b bonded with a piezoelectric layer of the same length ($L_p = L$) and width as the beam and subjected to a concentrated force $P(t)$ as shown in Fig. 1. According to the Timoshenko beam theory, constituting equations are represented as

$$u(x,z,t) = u_0(x,t) - z\theta(x,t), \quad w(x,z,t) = w_0(x,t), \tag{1}$$

$$\sigma_x = E\varepsilon_x, \quad \tau_{xz} = \kappa G\gamma_{xz}, \quad \varepsilon_x = \partial u_0/\partial x - z\partial\theta/\partial x, \quad \gamma_{xz} = \partial w_0/\partial x - \theta, \tag{2}$$

where $u(x,z,t), w(x,z,t)$ are axial and transverse displacements at arbitrary point in cross-section at x and $u_0(x,t), w_0(x,t)$ are the displacements on the neutral plane; θ is cross-section rotation; $\varepsilon_x, \gamma_{xz}, \sigma_x, \tau$ are deformation and strain components; κ is geometry correction factor.

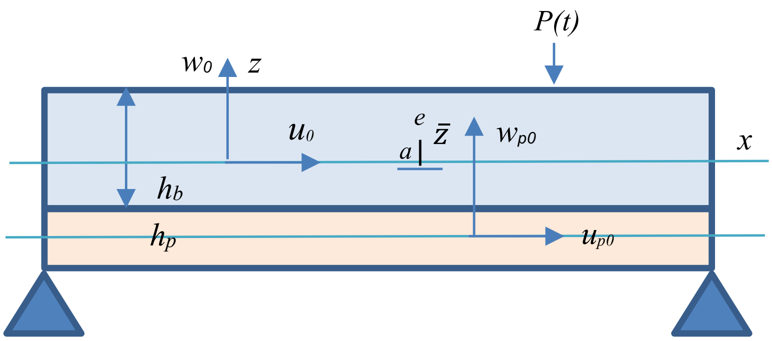

Fig. 1. Cracked Timoshenko beam with piezoelectric layer under concentrated force

Governing equations for the piezoelectric layer treated as a homogeneous Timoshenko beam element are

$$\begin{gathered} u_p(x,\bar{z},t) = u_{p0}(x,t) - \bar{z}\theta_p(x,t), \quad w_p(x,\bar{z},t) = w_{p0}(x,t), \\ \varepsilon_{px} = u'_{p0} - \bar{z}\theta'_p, \quad \gamma_p = w'_{p0} - \theta_p, \\ \sigma_{px} = C^p_{11}\varepsilon_{px} - h_{13}D, \quad \tau_p = C^p_{55}\gamma_p, \quad \epsilon = -h_{13}\varepsilon_{px} + \beta^p_{33}D, \end{gathered} \tag{3}$$

where C^p_{11}, C^p_{55} are elastic and shear modulus, h_{13}, β^p_{33} are piezoelectric and dielectric constants; ϵ and D are electric field and displacement of the piezoelectric material.

Assume that the base beam and piezoelectric layer are perfectly bonded, and they have the same cross-section rotation so that it should be satisfied the conditions

$$u\left(x, -\frac{h_b}{2}, t\right) = u_p\left(x, \frac{h_p}{2}, t\right), \quad w(x, -h_b/2,) = w_p(x, h_p/2, t), \quad \theta = \theta_p, \tag{4}$$

that yield

$$\begin{gathered} u_{p0} = u_0 + \theta h, \quad h = \left(h_b + h_p\right)/2, \quad w_{p0} = w_0\,, \\ \varepsilon_{px} = u_0' - \left(\bar{z} - h\right)\theta', \quad \gamma_p = w_0' - \theta. \end{gathered} \tag{5}$$

Therefore, strain and kinetic energies of the integrated beam can be calculated as

$$\Pi = \Pi_b + \Pi_p = (1/2)\int_0^L \left\{ \begin{array}{c} A_{11}^* u_0'^2 + 2A_{12}^* u_0'\theta' + A_{22}^*\theta'^2 + A_{33}^*\left(w_0' - \theta\right)^2 \\ -2h_{13}A_p D\left(u_0' + h\theta'\right) + \beta_{33}^p A_p D^2 \end{array} \right\} \mathrm{d}x, \tag{6}$$

$$T = T_p + T_p = (1/2)\int_0^L \left\{ I_{11}^* \dot{u}_0^2 + 2I_{12}^* \dot{u}_0 \dot{\theta} + I_{22}^* \dot{\theta}^2 + I_{11}^* \dot{w}_0^2 \right\} \mathrm{d}x, \tag{7}$$

where comma and dot denote derivative with respect to x and t respectively and

$$\begin{gathered} A_{11}^* = EA_b + C_{11}^p A_p\,, \quad A_{12}^* = C_{11}^p A_p h, \quad A_{22}^* = EI_b + C_{11}^p\left(I_p + A_p h^2\right), \\ A_{33}^* = \kappa G A_b + C_{55}^p A_p\,, \quad I_{11}^* = \rho_b A_b + \rho_p A_p, \quad I_{12}^* = \rho_p A_p h, \quad I_{22}^* = \rho_b I_b + \rho_p I_p + \rho_p A_p h^2, \\ A_b = bh_b, \quad A_p = bh_p, \quad I_b = bh_b^3/12, \quad I_p = bh_p^3/12. \end{gathered} \tag{8}$$

The work done by transverse force $P\left(t\right)$ applied at the position x_0 on the beam is

$$W = \int_0^L P\left(t\right)\delta\left(x - x_0\right) w_0\left(x,t\right) \mathrm{d}x, \tag{9}$$

where $\delta\left(x\right)$ is Dirac's function. Substituting expressions (6), (7) and (9) into the Hamilton's principle

$$\int_{t_1}^{t_2} \delta\left(T - \Pi + W\right) \mathrm{d}t = 0, \tag{10}$$

yields

$$\begin{gathered} \left(I_{11}^*\ddot{u}_0 - A_{11}^* u_0''\right) + \left(I_{12}^*\ddot{\theta} - A_{12}^*\theta''\right) + h_{13}A_p D' = 0, \\ \left(I_{12}^*\ddot{u}_0 - A_{12}^* u_0''\right) + \left(I_{22}^*\ddot{\theta} - A_{22}^*\theta''\right) - A_{33}^*\left(w_0' - \theta\right) + h_{13}A_p h D' = 0, \\ I_{11}^*\ddot{w}_0 - A_{33}^*\left(w_0'' - \theta'\right) = P\left(t\right)\delta\left(x - x_0\right), \quad h_{13}A_p\left(u_0' + h\theta'\right) - \beta_{33}^p A_p D = 0. \end{gathered} \tag{11}$$

Obviously, from the last equation in (11) one finds

$$D = h_{13}\left(u_0' + h\theta'\right)/\beta_{33}^p\,, \tag{12}$$

that allows the remaining equations to be rewritten as

$$\begin{gathered} \left(I_{11}^*\ddot{u}_0 - B_{11}^* u_0''\right) + \left(I_{12}^*\ddot{\theta} - B_{12}^*\theta''\right) = 0, \\ \left(I_{12}^*\ddot{u}_0 - B_{12}^* u_0''\right) + \left(I_{22}^*\ddot{\theta} - B_{22}^*\theta''\right) - A_{33}^*\left(w_0' - \theta\right) = 0, \\ I_{11}^*\ddot{w}_0 - A_{33}^*\left(w_0'' - \theta'\right) = P\left(t\right)\delta\left(x - x_0\right), \end{gathered} \tag{13}$$

where

$$\begin{gathered} B_{11}^* = A_{11}^* - A_p h_{13}^2/\beta_{33}^p = EA_b + E_p A_p, \quad B_{12}^* = A_{12}^* - A_p h h_{13}^2/\beta_{33}^p = E_p A_p h, \\ B_{22}^* = A_{22}^* - A_p h^2 h_{13}^2/\beta_{33}^p = EI_b + C_{11}^p I_p + E_p A_p h^2, \quad E_p = C_{11}^p - h_{13}^2/\beta_{33}^p. \end{gathered} \tag{14}$$

In case of external harmonic force, $P(t) = P_0 \exp\{i\omega t\}$, seeking solution of Eq. (13) in the form

$$\{u_0(x,t), \theta(x,t), w_0(x,t)\} = \{U(x,\omega), \theta(x,\omega), W(x,\omega)\} \exp\{i\omega t\}, \tag{15}$$

that leads the equations to

$$[\mathbf{A}]\{\mathbf{Z}''(x,\omega)\} + [\mathbf{B}]\{\mathbf{Z}'(x,\omega)\} + [\mathbf{C}]\{\mathbf{Z}(x,\omega)\} = \{\mathbf{P}(x,\omega)\}, \tag{16}$$

$$\mathbf{Z}' = \mathrm{d}\mathbf{Z}/\mathrm{d}x,\ \mathbf{Z}'' = \mathrm{d}^2\mathbf{Z}/\mathrm{d}x^2,\ \mathbf{P}(x,\omega) = \{0, 0, Q(x,x_0)\}^T,\ Q(x,x_0) = P_0\delta(x-x_0), \tag{17}$$

with the matrices

$$[\mathbf{A}] = \begin{bmatrix} B_{11}^* & B_{12}^* & 0 \\ B_{12}^* & B_{22}^* & 0 \\ 0 & 0 & A_{33}^* \end{bmatrix}, \quad [\mathbf{B}] = \begin{bmatrix} 0 & 0 & 0 \\ 0 & 0 & A_{33}^* \\ 0 & -A_{33}^* & 0 \end{bmatrix},$$

$$[\mathbf{C}] = \begin{bmatrix} \omega^2 I_{11}^* & \omega^2 I_{12}^* & 0 \\ \omega^2 I_{12}^* & \omega^2 I_{22}^* - A_{33}^* & 0 \\ 0 & 0 & \omega^2 I_{11}^* \end{bmatrix}.$$

Also, putting expression (15) into (12) and calculating electric charge produced in the piezoelectric layer under vibration of beam allow one to obtain

$$Q(t) = \int_0^L D(x,t)\, b\mathrm{d}x = Q_p(\omega) \exp\{i\omega t\}, \tag{18}$$

where

$$Q_p(\omega) = \left(bh_{13}/\beta_{33}^p\right) \int_0^L \left[U'(x,\omega) + h\Theta'(x,\omega)\right] \mathrm{d}x. \tag{19}$$

The latter function $Q_p(\omega)$ is acknowledged as electrical frequency response of the beam to the concentrated load.

Assume furthermore that a crack of depth a occurs at position e in the host beam and crack is represented by a pair of equivalent springs: translational spring of stiffness T and rotational one of stiffness R. Thus, conditions should be satisfied at the crack position are

$$\begin{gathered} U(e+0) = U(e-0) + \gamma_a U'_x(e), \quad \Theta(e+0) = \Theta(e-0) + \gamma_b \Theta'_x(e), \\ W(e+0) = W(e-0), \quad U'_x(e+0) = U'_x(e-0), \\ \Theta'_x(e+0) = \Theta'_x(e-0), \quad W'_x(e+0) = W'_x(e-0) + \gamma_b \Theta'_x(e), \end{gathered} \tag{20}$$

where $\gamma_a = EA/T, \gamma_b = EI_b/R$ are calculated from crack depth a for axial [19] and flexural [20] vibrations as

$$\gamma_a = 2\pi\left(1-\nu_0^2\right) h_b f_a(z), \quad \gamma_b = 6\pi\left(1-\nu_0^2\right) h_b f_b(z), \quad z = a/h_b, \tag{21}$$

$$\begin{aligned} f_1(z) &= z^2\Big(0.6272 - 0.17248z + 5.92134z^2 - 10.7054z^3 + 31.5685z^4 - 67.47z^5 \\ &\quad + 139.123z^6 - 146.682z^7 + 92.3552z^8\Big), \\ f_2(z) &= z^2\Big(0.6272 - 1.04533z + 4.5948z^2 - 9.9736z^3 + 20.2948z^4 - 33.0351z^5 \\ &\quad + 47.1063z^6 - 40.7556z^7 + 19.6z^8\Big). \end{aligned} \tag{22}$$

3. FREQUENCY RESPONSE FUNCTION OF CRACKED BEAM WITH PIEZOELECTRIC LAYER

It is well-known from the theory of differential equations that general solution of inhomogeneous equation (16) is composed from general solution of homogeneous equation and a particular solution of the inhomogeneous one

$$\{\mathbf{Z}(x,\omega)\} = \{\mathbf{Z}_0(x,\omega)\} + \{\mathbf{Z}_q(x,\omega)\}, \tag{23}$$

where $\{\mathbf{Z}_q(x,\omega)\} = \{U_q(x,\omega), \Theta_q(x,\omega), W_q(x,\omega)\}^T$ is a particular solution of inhomogeneous equations (16) and $\{\mathbf{Z}_0(x,\omega)\}$ is general solution of homogeneous equations, an explicit expression of which was conducted in Ref. [21] for cracked beam as

$$\{\mathbf{Z}_0(x,\omega)\} = [\mathbf{\Phi}(x,\omega)]\{\mathbf{C}\}, \tag{24}$$

with constant vector $\{\mathbf{C}\} = \{C_1, \ldots, C_6\}^T$ and matrices

$$[\mathbf{\Phi}(x,\omega)] = \left[\mathbf{G}_0(x,\omega) + \mathbf{K}(x-e)\,\mathbf{G}_0'(x,\omega)\right], \tag{25}$$

$$[\mathbf{K}(x)] = \begin{cases} [\mathbf{G}_c(x)] & : x > 0, \\ [\mathbf{0}] & : x \le 0, \end{cases} \qquad [\mathbf{K}'(x)] = \begin{cases} [\mathbf{G}_c'(x)] & : x > 0, \\ [\mathbf{0}] & : x \le 0. \end{cases}$$

Matrices $\mathbf{G}_0(x,\omega)$ and $\mathbf{G}_c(x)$ are given in Appendix A. Also, according to the theory of differential equations, particular solution $\{\mathbf{Z}_q(x,\omega)\}$ can be found in in the form

$$\{\mathbf{Z}_q(x,\omega)\} = \int_0^x [\mathbf{H}(x-\tau)]\{\mathbf{P}(\tau,\omega)\}\,\mathrm{d}\tau = P_0\{\mathbf{h}_3(x-x_0)\}, \tag{26}$$

where vector function $\mathbf{h}_3(x) = \{h_{31}(x), h_{32}(x), h_{33}(x)\}^T$ is the third column vector of matrix $\mathbf{H}(x)$ defined as solution of equation

$$[\mathbf{A}]\left[\mathbf{H}''(x)\right] + [\mathbf{B}] + [\mathbf{C}][\mathbf{H}(x)] = \{\mathbf{0}\}, \quad [\mathbf{H}(0)] = [\mathbf{0}], \quad [\mathbf{A}]\left[\mathbf{H}'(0)\right] = [\mathbf{I}_3]. \tag{27}$$

Using expression (24), the vector function $\mathbf{h}_3(x)$ as a component solution of Eq. (27) can be found as

$$\{\mathbf{h}_3(x)\} = \left[\overline{\mathbf{H}}(x)\right]\{\mathbf{d}\}, \tag{28}$$

with matrix $\overline{\mathbf{H}}(x)$ and vector $\mathbf{d}$ given in Appendix B.

Constant vector $\{\mathbf{C}\}$ is determined by given boundary conditions, for example of the simply supported beam, that are of the form

$$U(0) = W(0) = M(0) = N(L) = W(L) = M(L) = 0, \tag{29}$$

where $N(x) = B_{11}^{*}\partial_x U(x) - B_{12}^{*}\partial_x \Theta(x)$ $M(x) = B_{12}^{*}\partial_x U(x) - B_{22}^{*}\partial_x \Theta(x)$. Namely, in this case the vector is

$$\{\mathbf{C}\} = -P_0 \left[\mathbb{R}(\omega)\right]^{-1} \left\{\hat{\mathbf{P}}(\omega)\right\},$$

where

$$\begin{gathered} \hat{P}_1(\omega) = 0, \quad \hat{P}_2(\omega) = 0, \quad \hat{P}_3(\omega) = 0, \quad \hat{P}_6(\omega) = h_{33}(L - x_0), \\ \hat{P}_4(\omega) = \left[B_{11}^{*}h_{31}'(L - x_0) - B_{12}^{*}h_{32}'(L - x_0)\right], \\ \hat{P}_5(\omega) = \left[B_{12}^{*}h_{31}'(L - x_0) - B_{22}^{*}h_{32}'(L - x_0)\right], \end{gathered} \tag{30}$$

and

$$\mathbb{R}(\omega) = \begin{bmatrix} \alpha_1 & \alpha_2 & \alpha_3 & \alpha_1 & \alpha_2 & \alpha_3 \\ m_1 & m_2 & m_3 & -m_1 & -m_2 & -m_3 \\ \beta_1 & \beta_2 & \beta_3 & -\beta_1 & -\beta_2 & -\beta_3 \\ N_1(L) & N_2(L) & N_3(L) & N_4(L) & N_5(L) & N_6(L) \\ M_1(L) & M_2(L) & M_3(L) & M_4(L) & M_5(L) & M_6(L) \\ \phi_{31}(L) & \phi_{32}(L) & \phi_{33}(L) & \phi_{34}(L) & \phi_{35}(L) & \phi_{36}(L) \end{bmatrix}, \tag{31}$$

$$m_j = \left(B_{12}^{*}\alpha_j - B_{22}^{*}\right)k_j, \quad j = 1,2,3, \quad N_j(L) = B_{11}^{*}\phi_{1j}'(L) - B_{12}^{*}\phi_{2j}'(L),$$

$$M_j(L) = B_{12}^{*}\phi_{1j}'(L) - B_{22}^{*}\phi_{2j}'(L), \quad j = 1,2,\ldots,6,$$

$\phi_{ij}(x), \phi_{ij}'(x), i = 1,2,3; j = 1,2,\ldots,6$ are elements and their derivatives of matrix $\mathbf{\Phi}(x,\omega)$ defined in (A.2). Therefore, solution of Eq. (16) is finally found as

$$\{\mathbf{Z}(x,\omega)\} = \left\{\mathbf{Z}_q(x,\omega)\right\} - P_0\left[\mathbf{\Phi}(x,\omega)\right]\left[\mathbb{R}(\omega)\right]^{-1}\left\{\hat{\mathbf{P}}(\omega)\right\},$$

or

$$\{\mathbf{Z}(x,\omega)\} = P_0\left\{\mathbf{h}_3(x - x_0) - \left[\mathbf{\Phi}(x,\omega)\right]\left[\mathbb{R}(\omega)\right]^{-1}\left\{\hat{\mathbf{P}}(\omega)\right\}\right\}. \tag{32}$$

From latter equation one can obtain frequency response vector-function

$$\begin{aligned} \{MFRF(x,x_0,\omega)\} &= \{\mathbf{Z}(x,\omega)\}/P_0 \\ &= \{FU(x,x_0,\omega), F\Theta(x,x_0,\omega), FW(x,x_0,\omega)\}^T \\ &= \left\{\mathbf{h}_3(x - x_0) - \left[\mathbf{\Phi}(x,\omega)\right]\left[\mathbb{R}(\omega)\right]^{-1}\left\{\hat{\mathbf{P}}(\omega)\right\}\right\}, \end{aligned} \tag{33}$$

that is, as usually, called mechanical frequency response function of the integrated beam. Owning the mechanical frequency response function $\{MFRF(x,x_0,\omega)\}$, the corresponding output charge called herein electrical frequency response function can be calculated according to Eq. (19) as

$$
\begin{aligned}
EFRF\left(x_0,\omega\right) &= \left(bh_{13}/\beta_{33}^{p}\right)\int_0^L \left[FU'\left(x,x_0,\omega\right)+hF\Theta'\left(x,x_0,\omega\right)\right]\mathrm{d}x \\
&= \frac{bh_{13}}{\beta_{33}^{p}}\Big\{\left[FU\left(L,x_0,\omega\right)-FU\left(0,x_0,\omega\right)-\gamma_a FU'\left(e,\omega\right)\right] \\
&\quad + h\left[F\Theta\left(L,\omega\right)-F\Theta\left(0,\omega\right)-\gamma_b F\Theta'\left(e,\omega\right)\right]\Big\},
\end{aligned}
\tag{34}
$$

with crack magnitudes γ_a, γ_b defined above in Eqs. (21)–(22). The obtained above electrical frequency response function is the subject of numerical analysis accomplished in consequent section.

4. NUMERICAL RESULTS AND DISCUSSION

Let's consider the coherence between two frequency-dependent signals $S_1\left(\omega\right)$ and $S_2\left(\omega\right)$ defined in a frequency segment $\left[\omega_a,\omega_b\right]$ likely the modal assurance criterion [22, 23]

$$
SI=\sum_{k=1}^{N} S_1\left(\omega_k\right)S_2\left(\omega_k\right)\Bigg/\left[\sum_{k=1}^{N} S_1^2\left(\omega_k\right)\cdot\sum_{k=1}^{N} S_2^2\left(\omega_k\right)\right]^{1/2}. \tag{35}
$$

This index lies between 0 and 1 and that equals 1 only if the two signals are fully similar, so that it can be used for checking similarity of two functional signals and called similarity index. Two given signals may be acknowledged as similar if the index calculated by Eq. (35) is close to 1, for example, equals 0.999.

For analysis of the effect of crack on the electrical frequency response function given by Eq. (35), let's to introduce so-called spectral damage index calculated from a pair of frequency-dependent signals $\hat{Q}\left(\omega,e,a\right)$, $\hat{Q}^0\left(\omega\right)$ measured respectively for cracked and intact beams [18]

$$
SDI\left(e,a\right)=\sum_{k=1}^{N}\hat{Q}\left(\omega_k,e,a\right)\hat{Q}^0\left(\omega\right)\Bigg/\left[\sum_{k=1}^{N}\hat{Q}^2\left(\omega_k,e,a\right)\cdot\sum_{k=1}^{N}\hat{Q}^{02}\left(\omega_k\right)\right]^{1/2}. \tag{36}
$$

Hence, deviation of the damage index from 1 represents a measure of the crack effect on the index, and as usual, it is acknowledged as the sensitivity of the signal under consideration to crack. Note, if the compared signals are the electric frequency response functions of the intact and cracked beam, $EFRF\left(x_0,\omega,e,a\right)$, $EFRF\left(x_0,\omega\right)$, the spectral damage index is dependent also on the location where the concentrated load is applied x_0, e.g. $SDIEF=SDI\left(x_0,e,a\right)$.

SDIEF in dependence upon crack parameters and applied load position is numerically examined bellow with the following geometry and material constants [24]

$$L_b = L_p = L = 1\text{ m}, b = 0.1\text{ m}, h_b = L/10,$$

$$E_t = 390\text{ MPa}, \rho_t = 3960\text{ kg/m}^3, \mu_t = 0.25; E_b = 210\text{ MPa}, \rho_b = 7800\text{ kg/m}^3, \mu_b = 0.31,$$

$$C_{11}^p = 69.0084\text{ GPa}, C_{55}^p = 21.0526\text{ GPa}, \rho_p = 7750\text{ kg/m}^3, h_{13} = -7.70394 \times 10^8\text{ V/m}.$$

Table 1. Similarity of Electrical and Mechanical (Midspan) Frequency Response functions for different load application positions and crack depth

Crack depth	Load application position, x_0								
	0.1	0.2	0.3	0.4	0.5	0.6	0.7	0.8	0.9
Uncrack	0.9991	0.9999	0.9993	0.9990	0.9993	0.9998	0.9999	0.9993	0.9986
0.1	0.9992	0.9999	0.9992	0.9991	0.9992	0.9998	0.9999	0.9993	0.9985
0.2	0.9997	0.9993	0.9992	0.9993	0.9991	0.9998	0.9998	0.9992	0.9984
0.3	0.9996	0.9988	0.9993	0.9996	0.9989	0.9998	0.9998	0.9992	0.9983
0.4	0.9983	0.9990	0.9996	0.9997	0.9987	0.9998	0.9998	0.9991	0.9982
0.5	0.9993	0.9997	0.9997	0.9988	0.9985	0.9998	0.9998	0.9990	0.9981
$e/L = 0.5, h_p/h_b = 0.1$									

Table 2. Similarity of Electrical and Mechanical (Midspan) Frequency Response functions in different piezoelectric layer thickness and crack depth

Crack depth	Piezoelectric layer thickness, h_p/h_b								
	0.01	0.05	0.08	0.10	0.12	0.15	0.20	0.25	0.30
Uncrack	0.9991	0.9992	0.9992	0.9993	0.9993	0.9993	0.9993	0.9994	0.9994
0.1	0.9991	0.9991	0.9992	0.9992	0.9992	0.9993	0.9993	0.9993	0.9993
0.2	0.9989	0.9990	0.9990	0.9991	0.9991	0.9991	0.9992	0.9992	0.9993
0.3	0.9987	0.9988	0.9989	0.9989	0.9989	0.9990	0.9990	0.9991	0.9991
0.4	0.9984	0.9985	0.9986	0.9987	0.9987	0.9988	0.9988	0.9989	0.9990
0.5	0.9982	0.9983	0.9984	0.9985	0.9985	0.9986	0.9987	0.9988	0.9988
Crack location, $e/L = 0.5$; Load application position, $x_0 = 0.5$									

First, similarity of electrical ($EFRF\,(x_0, \omega)$) and mechanical midspan ($MFRF\,(L/2, x_0, \omega)$) frequency response functions is checked by using Eq. (35) and results are presented in Tables 1, 2 for various crack depth, loading location and piezoelectric layer thickness with given crack location at beam midspan $e/L = 0.5$. Evidently, similarity of MFRF and EFRF is well ensured for uncracked beam independently upon loading position and distributed sensor thickness less than 30% beam thickness. In case of cracked beam crack depth may slightly reduce the similarity index of the FRFs and the best choosing the sensor thickness shows to be 10% of beam thickness.

Fig. 2 demonstrates the spectral damage index of electrical frequency response function (EFRF) as a function of normalized crack location e/L with various relative crack depth a/h in case of load applied at the beam middle, $x_0 = L/2$. It can be seen that the change in the EFRF due to crack location is similar to the variation of the first natural frequency which reaches the maximum for the crack occurred at the beam middle. However, the change due to crack depth increases significantly in magnitude compared to the natural frequency. This means the EFRF is much more sensitive to cracks than natural frequencies.

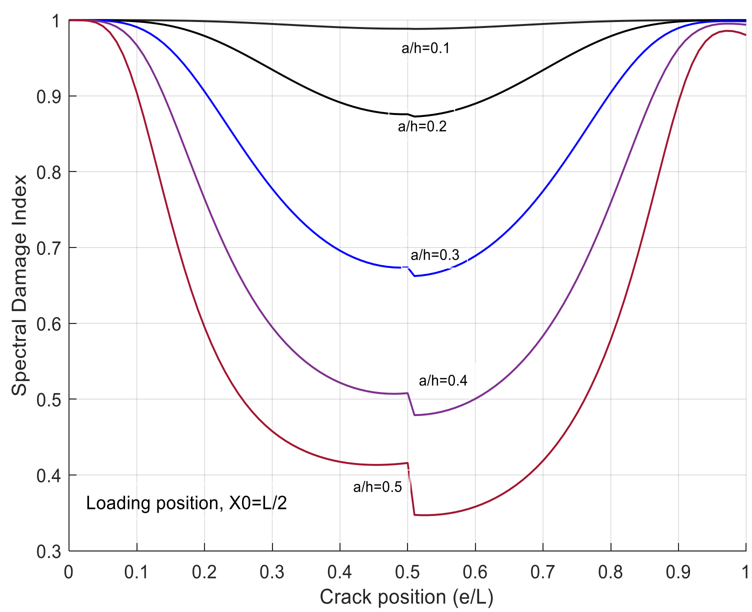

Fig. 2. Spectral damage index versus crack location in various crack depth, $x_0 = L/2$

There are depicted in Fig. 3 spectral damage index versus crack location in different position of load applied at the positions $x_0/L = 0.3$ and 0.7 with fixed crack depth $a/h = 0.3$. The effect of loading location on the crack-induced change in EFRF is noticeably distinguished only when the crack appears at positions between loading site and crack depth reaching 30% beam depth (Fig. 4). The sensitivity of EFRF loaded at position x_0 to crack undergoes an abrupt change at location $L - x_0$ which may be explained by the discontinuity of response to a concentrated point load. Therefore, it can be concluded that the loads applied at the symmetric positions produce different sensitivity of EFRF only to crack appeared at the positions between the loading locations. Fig. 5 shows the

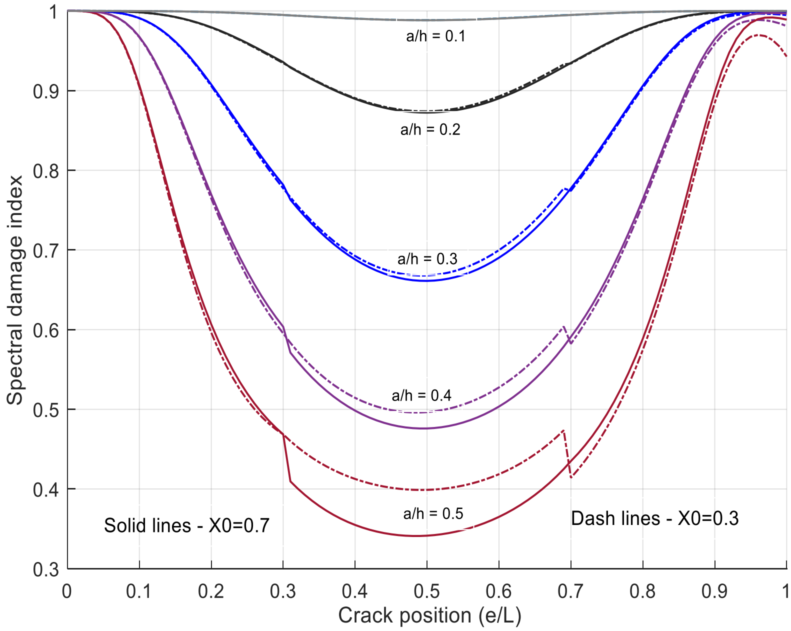

Fig. 3. Spectral damage index versus crack location in various loading position, $a/h = 0.3$

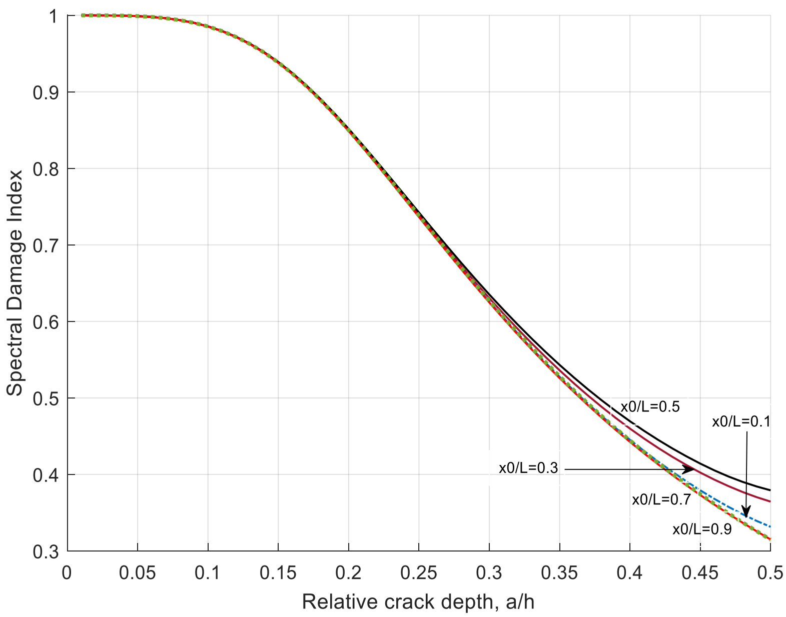

Fig. 4. Spectral damage index versus crack depth in various loading location x_0, $e/L = 0.5$

effect of piezoelectric layer thickness on sensitivity of EFRF to crack, that reveals monotonic increase of the EFRF sensitivity to crack with piezoelectric layer thickness until it is less than 15% of the beam thickness. The sensitivity starts decreasing for the layer thickness further growing from $0.15h_b$, especially, the sensitivity gets losing a half for the thickness increases from 20% to 25% of beam thickness. In all the Figures we can see the nonsmoothed variation of the spectral damage index which might be caused by the discontinuity of beam response to the concentrated force.

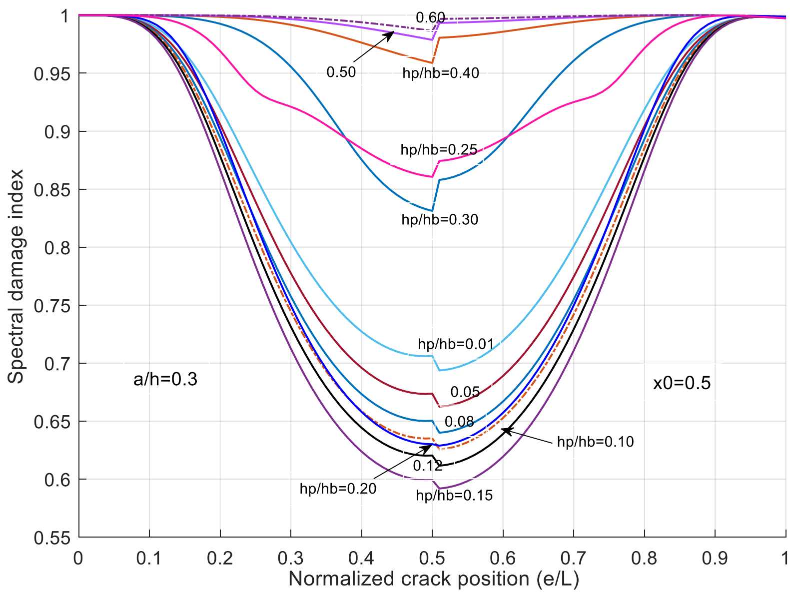

Fig. 5. Spectral damage index versus crack location in various thickness of piezoelectric layer, $x_0/L = 0.5$

5. CONCLUDING REMARKS

Thus, a new concept of frequency response function (FRF), called electrical frequency response function (EFRF) has been proposed in this report for a cracked Timoshenko beam bonded with a piezoelectric layer. This new concept of FRF is defined as the output charge produced in the piezoelectric layer immediately together with the mechanical frequency response function (MFRF).

The EFRF shows to be similar to the MFRF measured at the beam middle that confirms reliable utilization of piezoelectric layer as a distributed smart sensor for measuring mechanical response functions of a cracked beam structure. Moreover, there is conducted a representation of the EFRF explicitly expressed through crack parameters that provides a useful instrument for solving crack detection problem by using distributed piezoelectric sensor.

The effect of cracks on EFRF has been examined by using the so-called spectral damage index defined as the similarity index of EFRFs for intact and cracked beams and acknowledged as the sensitivity of EFRF to crack. Numerical results show that the change in the spectral damage index is similar to the change in the first natural frequency due to crack but with much greater magnitude. This implies a much higher sensitivity of the EFRF to crack compared to that of natural frequencies.

It's interesting to note that the distributed piezoelectric sensor is useful for measuring EFRF highly sensitive to cracks only for its thickness should be less than 20% beam thickness. Otherwise, the smart sensor of greater thickness may restore a cracked beam so that the piezoelectric sensor cannot reveal the appearance of a crack.

The next study of the authors will focus on developing a procedure for crack detection in beam by measurement of electrical frequency response function.

DECLARATION OF COMPETING INTEREST

The authors declare that they have no known competing financial interests or personal relationships that could have appeared to influence the work reported in this paper.

ACKNOWLEDGEMENT

This research has been completed with support from the Institute of Mechanics, VAST under Project of number VCH.TX.01.2024.

REFERENCES

[1] H. Sohn, C. R. Farrar, F. M. Hemez, D. D. Shunk, D. W. Stinemates, B. R. Nadler, and J. J. Czarnecki. *A review of structural health monitoring literature: 1996–2001*. Los Alamos National Laboratory Report, (2003).

[2] W. Fan and P. Qiao. Vibration-based damage identification methods: A review and comparative study. *Structural Health Monitoring*, **10**, (2010), pp. 83–111. https://doi.org/10.1177/1475921710365419.

[3] R. Hou and Y. Xia. Review on the new development of vibration-based damage identification for civil engineering structures: 2010–2019. *Journal of Sound and Vibration*, **491**, (2021). https://doi.org/10.1016/j.jsv.2020.115741.

[4] Z. Wang, R. M. Lin, and M. K. Lim. Structural damage detection using measured FRF data. *Computer Methods in Applied Mechanics and Engineering*, **147**, (1997), pp. 187–197. https://doi.org/10.1016/s0045-7825(97)00013-3.

[5] S. K. Thyagarajan, M. J. Schulz, P. F. Pai, and J. Chung. Detecting structural damage using frequency response functions. *Journal of Sound and Vibration*, **210**, (1998), pp. 162–170. https://doi.org/10.1006/jsvi.1997.1308.

[6] R. P. C. Sampaio, N. M. M. Maia, and J. M. M. Silva. Damage detection using the frequency-response-function curvature method. *Journal of Sound and Vibration*, **226**, (1999), pp. 1029–1042. https://doi.org/10.1006/jsvi.1999.2340.

[7] U. Lee and J. Shin. A frequency response function-based structural damage identification method. *Computers & Structures*, **80**, (2002), pp. 117–132. https://doi.org/10.1016/s0045-7949(01)00170-5.

[8] N.-G. Park and Y.-S. Park. Damage detection using spatially incomplete frequency response functions. *Mechanical Systems and Signal Processing*, **17**, (2003), pp. 519–532. https://doi.org/10.1006/mssp.2001.1423.

[9] H. Y. Hwang and C. Kim. Damage detection in structures using a few frequency response measurements. *Journal of Sound and Vibration*, **270**, (2004), pp. 1–14. https://doi.org/10.1016/s0022-460x(03)00190-1.

[10] X. Liu, N. A. J. Lieven, and P. J. Escamilla-Ambrosio. Frequency response function shape-based methods for structural damage localisation. *Mechanical Systems and Signal Processing*, **23**, (2009), pp. 1243–1259. https://doi.org/10.1016/j.ymssp.2008.10.002.

[11] M. Dilena, M. P. Limongelli, and A. Morassi. Damage localization in bridges via the FRF interpolation method. *Mechanical Systems and Signal Processing*, **52–53**, (2015), pp. 162–180. https://doi.org/10.1016/j.ymssp.2014.08.014.

[12] E. F. Crawley and J. de Luis. Use of piezoelectric actuators as elements of intelligent structures. *AIAA Journal*, **25**, (1987), pp. 1373–1385. https://doi.org/10.2514/3.9792.

[13] H. S. Tzou and C. I. Tseng. Distributed piezoelectric sensor/actuator design for dynamic measurement/control of distributed parameter systems: A piezoelectric finite element approach. *Journal of Sound and Vibration*, **138**, (1990), pp. 17–34. https://doi.org/10.1016/0022-460x(90)90701-z.

[14] D. Wang, H. Song, and H. Zhu. Electromechanical impedance analysis on piezoelectric smart beam with a crack based on spectral element method. *Mathematical Problems in Engineering*, **2015**, (2015), pp. 1–13. https://doi.org/10.1155/2015/713501.

[15] W. Na and J. Baek. A review of the piezoelectric electromechanical impedance based structural health monitoring technique for engineering structures. *Sensors*, **18**, (2018). https://doi.org/10.3390/s18051307.

[16] T. Wang, B. Tan, M. Lu, Z. Zhang, and G. Lu. Piezoelectric electro-mechanical impedance (EMI) based structural crack monitoring. *Applied Sciences*, **10**, (2020). https://doi.org/10.3390/app10134648.

[17] S. Bhalla and C.-K. Soh. Progress in structural health monitoring and non-destructive evaluation using piezo-impedance transducers. *Smart Materials and Structures: New Research, Nova Science Publishers, Inc., New York*, (2007), pp. 177–228.

[18] N. T. Khiem, T. T. Hai, L. K. Toan, N. T. Lan, and H. Q. Quyet. A novel criterion for crack detection in beam structures by frequency response functions. *Vietnam Journal of Mechanics*, **45**, (2023), pp. 273–286. https://doi.org/10.15625/0866-7136/19040.

[19] T. G. Chondros, A. D. Dimarogonas, and J. Yao. Longitudinal vibration of a continuous cracked bar. *Engineering Fracture Mechanics*, **61**, (1998), pp. 593–606. https://doi.org/10.1016/s0013-7944(98)00071-x.

[20] T. G. Chondros, A. D. Dimarogonas, and J. Yao. A continuous cracked beam vibration theory. *Journal of Sound and Vibration*, **215**, (1998), pp. 17–34. https://doi.org/10.1006/jsvi.1998.1640.

[21] T. T. Hai, P. T. Hang, and N. T. Khiem. A novel criterion for crack identification in beam-like structures using distributed piezoelectric sensor and controlled moving load. *Journal of Sound and Vibration*, **572**, (2024). https://doi.org/10.1016/j.jsv.2023.118155.

[22] R. J. Allemang. The modal assurance criterion–twenty years of use and abuse. *Sound and Vibration*, **37**, (8), (2003), pp. 14–23.

[23] E. J. Williams and A. Messina. Applications of the multiple damage location assurance criterion. *Key Engineering Materials*, **167–168**, (1999), pp. 256–264. https://doi.org/10.4028/www.scientific.net/kem.167-168.256.

[24] N. T. Khiem, T. T. Hai, and L. Q. Huong. Effect of piezoelectric patch on natural frequencies of Timoshenko beam made of functionally graded material. *Materials Research Express*, **7**, (2020). https://doi.org/10.1088/2053-1591/ab8df5.

APPENDIX A. EXPLICIT EXPRESSION OF GENERAL VIBRATION SHAPE FOR PIEZOELECTRIC BEAM

$$\{\mathbf{Z_0}(x,\omega)\} = [\mathbf{\Phi}(x,\omega)]\{\mathbf{C}\}, \tag{A.1}$$

where $\{\mathbf{C}\} = \{C_1, \dots, C_6\}^T$ is a constant vector and matrix $[\mathbf{\Phi}(x,\omega)]$ is

$$[\mathbf{\Phi}(x,\omega)] = \left[\mathbf{G}_0(x,\omega) + \mathbf{K}(x-e)\,\mathbf{G}_0'(e,\omega)\right], \tag{A.2}$$

$$[\mathbf{G}_0(x,\omega)] = \begin{bmatrix} \alpha_1 e^{k_1x} & \alpha_2 e^{k_2x} & \alpha_3 e^{k_3x} & \alpha_1 e^{-k_1x} & \alpha_2 e^{-k_2x} & \alpha_3 e^{-k_3x} \\ e^{k_1x} & e^{k_2x} & e^{k_3x} & e^{-k_1x} & e^{-k_2x} & e^{-k_3x} \\ \beta_1 e^{k_1x} & \beta_2 e^{k_2x} & \beta_3 e^{k_3x} & -\beta_1 e^{-k_1x} & -\beta_2 e^{-k_2x} & -\beta_3 e^{-k_3x} \end{bmatrix}, \tag{A.3}$$

$$[\mathbf{K}(x)] = \begin{cases} [\mathbf{G}_c(x)] & : x > 0, \\ [\mathbf{0}] & : x \le 0, \end{cases} \quad [\mathbf{K}'(x)] = \begin{cases} [\mathbf{G}_c'(x)] & : x > 0, \\ [\mathbf{0}] & : x \le 0, \end{cases} \tag{A.4}$$

$$[\mathbf{G}_c(x,\omega)] = \begin{bmatrix} \gamma_a \sum\limits_{i=1}^{3} \alpha_i \delta_{i1} \cosh k_i x & \gamma_b \sum\limits_{i=1}^{3} \alpha_i (\delta_{i2} + \delta_{i3}) \cosh k_i x & 0 \\ \gamma_a \sum\limits_{i=1}^{3} \delta_{i1} \cosh k_i x & \gamma_b \sum\limits_{i=1}^{3} (\delta_{i2} + \delta_{i3}) \cosh k_i x & 0 \\ \gamma_a \sum\limits_{i=1}^{3} \beta_i \delta_{i1} \sinh k_i x & \gamma_b \sum\limits_{i=1}^{3} \beta_i (\delta_{i2} + \delta_{i3}) \sinh k_2 x & 0 \end{bmatrix}, \tag{A.5}$$

$$\begin{gathered} \delta_{11} = (k_3\beta_3 - k_2\beta_2)/\Delta, \quad \delta_{12} = (\alpha_3 k_2 \beta_2 - \alpha_2 k_3 \beta_3)/\Delta, \quad \delta_{13} = (\alpha_2 - \alpha_3)/\Delta, \\ \delta_{21} = (k_1\beta_1 - k_3\beta_3)/\Delta, \quad \delta_{22} = (\alpha_1 k_3 \beta_3 - \alpha_3 k_1 \beta_1)/\Delta, \quad \delta_{23} = (\alpha_3 - \alpha_1)/\Delta, \\ \delta_{31} = (k_2\beta_2 - k_1\beta_1)/\Delta, \quad \delta_{32} = (\alpha_2 k_1 \beta_1 - \alpha_1 k_2 \beta_2)/\Delta, \quad \delta_{33} = (\alpha_1 - \alpha_2)/\Delta, \\ \Delta = k_1\beta_1(\alpha_2 - \alpha_3) + k_2\beta_2(\alpha_3 - \alpha_1) + k_3\beta_3(\alpha_1 - \alpha_2), \\ \alpha_j = \left(\omega^2 I_{11}^* + k_j^2 B_{11}^*\right) / \left(\omega^2 I_{12}^* + k_j^2 B_{12}^*\right), \quad \beta_j = k_j A_{33}^* / \left(\omega^2 I_{11}^* + k_j^2 A_{33}^*\right), \\ k_j = \sqrt{\eta_j}, \quad j = 1, 2, 3. \end{gathered} \tag{A.6}$$

with η_1, η_2, η_3 being roots of the characteristic equation $\det\left[\lambda^2\mathbf{A} + \lambda\mathbf{B} + \mathbf{C}\right] = 0$.

APPENDIX B. PARTICULAR SOLUTION IN FORCED VIBRATION OF PIEZOELECTRIC BEAM

$$\{\mathbf{H}_3(x)\} = \left[\overline{\mathbf{H}}(x)\right]\{\mathbf{d}\}, \tag{B.1}$$

with matrix

$$\left[\overline{\mathbf{H}}(x)\right] = \begin{bmatrix} \phi_{11}+\phi_{14} & \phi_{12}+\phi_{15} & \phi_{13}+\phi_{16} \\ \phi_{21}+\phi_{24} & \phi_{22}+\phi_{25} & \phi_{23}+\phi_{26} \\ \phi_{31}+\phi_{34} & \phi_{32}+\phi_{35} & \phi_{33}+\phi_{36} \end{bmatrix}, \tag{B.2}$$

and vector

$$\{\mathbf{d}\} = \left\{ \begin{matrix} \alpha_2-\alpha_3 & \alpha_3-\alpha_1 & \alpha_1-\alpha_2 \end{matrix} \right\}^T / D, \tag{B.3}$$

where

$$D = 2A_{33}\left[\beta_1 k_1(\alpha_2-\alpha_3) + \beta_2 k_2(\alpha_3-\alpha_1) + \beta_3 k_3(\alpha_1-\alpha_2)\right], \tag{B.4}$$

and $\phi_{jk}, j = 1,2,3; k = 1,2,\ldots,6$ are elements of matrix $[\mathbf{\Phi}(x,\omega)]$ given above by Eq. (A.2).